Journal of Aerosol Science 112 (2017) 1–10

Contents lists available at ScienceDirect

Journal of Aerosol Science

journal homepage: www.elsevier.com/locate/jaerosci

Performance calibration of low-cost and portable particular matter (PM) sensors

Di Liu[a], Qiang Zhang[b], Jingkun Jiang[b], Da-Ren Chen[a,*]

[a] Particle Laboratory, Department of Mechanical and Nuclear Engineering, Virginia Commonwealth University, 401 West Main Street, Richmond, VA 23284, United States

[b] Division of Air Pollution Control, School of Environment, Tsing Hua University, 30 Shuangqing Rd, Haidian Qu, Beijing Shi 100084, China

ARTICLE INFO

Keywords:
PM sensors
Low-cost sensors
Particulate matter (PM) monitoring
PM sensor calibration

ABSTRACT

In this study, we calibrated the performance of low-cost and portable PM sensors under the condition of steady-state particle mass concentration by challenging them with lab-generated particles in different size distributions and compositions. Tested PM sensors included four low-cost optical sensors, i.e., Sharp, Shinyei, Samyoung and Oneair, TSI DustTrak and Personal Dust Monitor (PDM). A scientific Tapered Element Oscillating Microbalance (TEOM; Thermal Scientific Model 1405) was applied as the reference. Same as what concluded in previous studies, our calibration data show that the readouts of all tested PM sensors had linear relationships with the particle mass concentration when the size distribution and composition of test particles were kept unchanged. However, the linear calibration lines for four low-cost PM sensors and DustTrak are different when the size distribution (i.e., mean size and geometrical standard deviation) and composition of particles were varied. The PDM output in general agreed well with that of reference TEOM for particles with mass concentration higher than 300 μg/m^3. The PDM, however, lost its sensitivity for measuring particles in the mass concentration less than 300 μg/m^3. Our study also demonstrated that the calibration of low-cost PM sensors should be performed under the condition of steady particle mass concentration instead of under the condition of transient particle concentration, even at very slow transient situation.

1. Introduction

The increasing awareness of adverse effect on the public health, caused by the exposure to particular matter (PM) in highly-polluted countries, such as China and India, has motivated the recent development of portable and personal sensors for monitoring the mass concentration of $PM_{2.5}$ (defined as PM with the particle sizes less than 2.5 μm, i.e., fine particles). Sources of fine PM are present in our daily life, e.g., in industrial discharge, vehicle exhaust and commercial kitchen emission. The mass concentration of fine PM has been linked to the frequent occurrence of asthma, particularly for children and elders (Fan, Li, Fan, Bai, & Yang, 2015; Norris et al., 1999), and the cardiovascular-disease-related mortality and mortality (Brook et al., 2010). The increased rate of lung cancer cases has also been associated with the increased exposure of fine particles (Borm, Schins, & Albrecht, 2004; Cohen & Pope, 1995; Knaapen, Borm, Albrecht, & Schins, 2004; Nyberg et al., 2000; Tie, Wu, & Brasseur, 2009). In addition to its adverse public health effect, fine PM, once released, also increased the environmental burden (Dockery et al., 1993; Evans et al., 2013; Krewski, 2009; Potera, 2014).

Scientific instruments for measuring PM mass concentration are readily available in market. They are in general large in their

* Corresponding author.
E-mail address: dechen3@vcu.edu (D.-R. Chen).

http://dx.doi.org/10.1016/j.jaerosci.2017.05.011
Received 8 March 2017; Received in revised form 17 May 2017; Accepted 22 May 2017
Available online 25 May 2017

final packages and expensive for the ownership. As a result, it is not feasible to apply these scientific instruments for simultaneously monitoring the PM concentration at multiple sites. Monitoring the spatial distribution of PM in time for providing a better picture on the transient particle pollution status are required in recent air pollution study and control (Gao, Cao, & Seto, 2015). More, the better correlation of PM exposure to related-heath data in epidemiology study requires the measurement of PM exposure at the personal level. PM sensors in small packages and at low cost are thus in high demand.

Filter-based samplers are reliable devices for measuring the mass concentration of PM in the ambience. The requirement of offline gravimetric analysis to get the final particle mass concentration data makes them inconvenient and time-consuming in use. Direct-reading PM sensors, based on either the mechanical or optical operation principle, have thus been developed (Roessler, 1982). Examples of mechanical PM monitors are the quartz crystal microbalance (QCM) (Alder & McCallum, 1983) and Tapered Element Oscillating Microbalance (TEOM) (Patashnick & Rupprecht, 1991). These mechanical monitors can be of high accuracy and independent of the size distribution and composition of PM. Photometers/nephelometers are representative instruments based on the light scattering. The simple configuration and continuous miniaturization/reduction of key components' makes optical PM sensors light in weight, compact in sizes and low in cost. Unfortunately, the performances of optical PM sensors are strongly dependent on the size distribution and composition of ambient particles.

Studies have been reported on the performance evaluation of low-cost optical PM sensors (Austin, Novosselov, Seto, & Yost, 2015; Holstius, Pillarisetti, Smith, & Seto, 2014; Sousan et al., 2016; Wang et al., 2015). All these studies reported a good linear relationship between the PM mass concentration and the responses of optical PM sensors. However, scanning mobility particle sizers (SMPSs), aerodynamic particle sizer (APS), SidePak or DustTrak was applied in these studies as the reference instruments for particle mass concentration measurement. SMPS/APS does not directly measure the mass concentration of PM. Instead, the mass concentration of PM was calculated from the measured number-based particle size distributions under the assumption that particles are spherical and particle density is known. More critically, the error associated with calculated mass concentration is often amplified in the calculation with small measurement error in the number-based particle size distribution measurement. For example, a 5% in number-based particle size distribution can easily result in at least 15% error in mass/volume-based particle size distribution. The above calculation error would be even higher if particles were agglomerates. The use of both SidePak and DustTrak as the reference are also problematic. It is because both are photometric sensors and all PM sensors evaluated in previous studies are based on the same operation principle. Further, some of previous studies carried out the evaluation under the condition with transient particle mass concentration. With the consideration of measuring cycles for a SMPS /APS, the time delay between the responses of reference and evaluated PM sensors could result in the potential error in the sensor performance calibration. It is thus necessary to perform the calibration of PM sensors via proper reference instruments and under the conditions of steady particle mass concentration.

In this study, the performance of four low-cost optical PM sensors, i.e., Sharp, Shinyei, Samyoung and Oneair, one Personal Dust Monitor (PDM; Thermal Scientific) and one DustTrak (TSI Inc.) were calibrated using lab-generated particles in the size distributions of different mean sizes, geometrical standard deviation and composition, and under the condition of steady-state particle concentration. The scientific TEOM (Model 1405) was applied as the reference instrument.

2. Sensors and calibration experiment

2.1. Tested PM sensors

Table 1 summarizes the specification of low-cost and portable PM sensors tested in this study. Four low-cost optical PM sensors, i.e., Shinyei PPD42NS, Samyoung DSM501A, Sharp GP2Y1010AU0F and Oneair CP-15-A4, were selected because of their popularity and compact sizes. All these low-cost optical PM sensors are based on light scattering technique. For the reference, the schematic configurations of four low-cost PM sensors, illustrating the aerosol openings and passage in each low-cost sensor, are given in Fig. 1. Fig. 1(a) is the basic configuration of Shinyei and Samyoung sensors (both sensors share the same configuration). The configurations of Sharp and Oneair sensors are in Fig. 1(b) and (c), respectively. Note that the solid lines in the diagrams represent the openings on the sensor cover surface. The shaded area in each diagram, are the potential space occupied by particles. In each of these low-cost

Table 1
Specification of low-cost sensors and portable PM sensors.

	Low-cost Sensors				**Portable Sensors**	
Sensor	Sharp	Shinyei	Samyoung	Oneair	Personal Dust Monitor	Dustrak
Model #	GP2Y1010AU0F	PPD42NS	DSM501A	CP-15-A4	PDM3700	8533
Size(mm)	46 × 30 × 18	59 × 45 × 22	59 × 45 × 20	45 × 35 × 23	243 × 172 × 83	135 × 216 × 224
Sampling method	Self diffusion	Thermal Convection	Thermal Convection	Active Sampling (Fan)	Pump sampling	Pump sampling
Detection Principle	Optical	Optical	Optical	Optical	Vibration	Optical
Detectable size range	N/A	~ 1.0 μm	~ 1.0 μm	0.3–10.0 μm	< 4.5 μm	PM_1, $PM_{2.5}$, PM_{10}, TSP
Concentration range	0.5 mg/m^3	28,000 #/L	1.4 mg/m^3	6 mg/m^3	200 mg/m^3	150 mg/m^3
Output signal	Analog output	Pulse width modulation	Pulse width modulation	Mass concentration	Mass concentration	Mass concentration

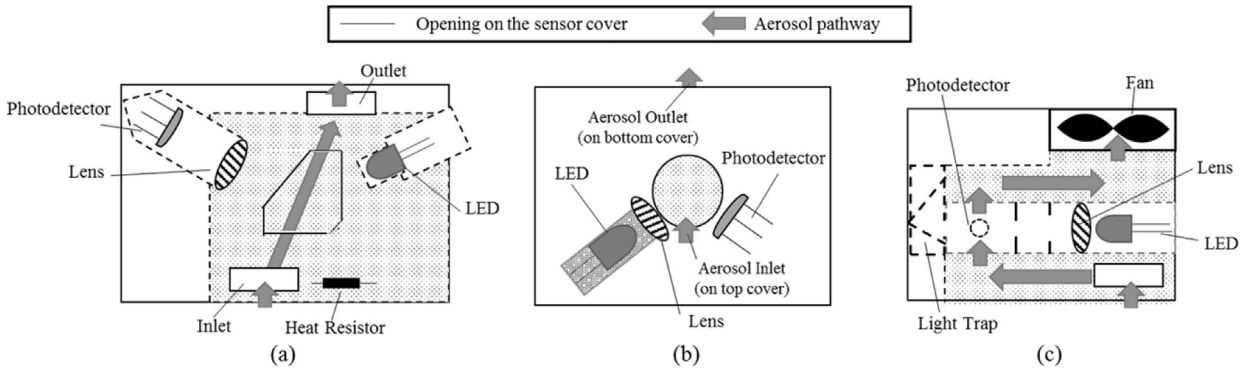

Fig. 1. Schematic diagram of the low-cost sensor: (a) for Shinyei (Or Samyoung) sensor; (b) for Sharp sensor; (c) for Oneair sensor.

sensors, an infrared (IR) emitting diode was used as the light source and a phototransistor as the detector for scattered lights. The scattering angles of these low-cost optical PM sensors are of 90–120°. As particles pass through the sensing volume, defined by the optical path of illumination light and viewing angle of the detector, the phototransistor measures photons scattered from particles once irradiated. Thermal-driven upwind flows are generated in both Shinyei and Samyoung PM sensors by electrically heating a resistor near the sensor inlet to sample particles through sensing volumes. As a result, above both sensors are instructed to install vertically with the inlet facing downward. Different from Shinyei and Samyoung sensors, an Oneair sensor has its own fan to move particles through its sensing volume. The Sharp sensor, however, only relies on the particle diffusion to move them through the sensor. An Arduino microcontroller was applied in our experiment to provide required voltages for the operation and the readout collection of all low-cost PM sensors.

The readout of the Sharp sensor is an analog signal from its photodetector. The Sharp sensor outputs higher voltage signal as more scattered photons reach its detector. The readout of Oneair sensor is based on its built-in calibration curve, obtained by calibrating it against the readout of Dustrak II 8530 (TSI Inc.) in the factory. Different from Sharp and Oneair sensors, the readouts of both Shinyei and Samyoung sensors are so-called pulse-width modulated (PWM), i.e., these PM sensors only output a “High” state when particles are not present in the sensing volumes and a “Low” state when particles were present. The mass concentration of particles in the sensing volume is assumed to correlate with the low pulse occupancy ratio, which is calculated as $\frac{\#\ of\ low\ state\ output}{total\ \#\ of\ state\ output}$.

A DustTrak DRX Aerosol Monitor (TSI Model 8522) was also included in this experiment. Similar to four low-cost optical PM

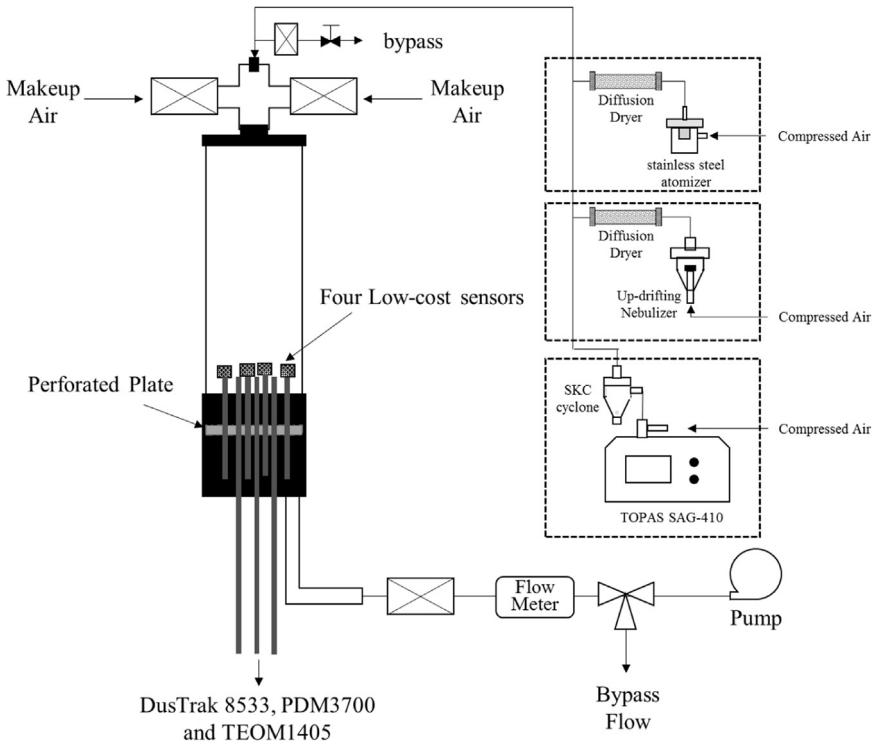

Fig. 2. Schematic diagram of the calibration setup used in this study.

sensors, the DustTrak DRX measures particle mass concentration via light scattering technique. It operates at a total sampling flowrate of 3.0 l/min (LPM), in which 1.0 LPM flow is filtered by a HEPA tube filter and used as sheath air. Different from IR emitting diodes in low-cost optical PM sensors, DustTrak DRX uses a laser diode with 655 nm in wavelength as its light source, and its light scattering angle is 90 ± 62°. A gold-coated spherical mirror is also included in the optical subsystem of DustTrak to collect the scattered photons in a wide angle and focus them onto its photodetector.

In addition to optical sensors, we included one mechanical PM sensor, i.e., Personal Dust Monitor (PDM model 3700; Thermo Fisher Scientific Inc.) in our study. The mechanical measurement principle of the PDM is the same as that of our reference instrument, i.e., tapered element oscillating microbalance, TEOM (Continuous Ambient Particulate Monitor, Model 1405, Thermo Fisher Scientific Inc.). Both TEOM 1405 and PDM 3700 capture particles on a small disk filter located at the tapored end of an oscillating element. A tapered glass tube is used as the oscillating element in the TEOM 1405, while a deformed metal tube is in the PDM 3700. As particles are collected on the disk filter, the mass increase of disk filter leads reduction on the vibrating frequency of tapered elements. PDM 3700 is a personal dust monitor for miners (by US NIOSH). The use of TEOM 1405 as the reference in our study is because it is a US EPA-approved instrument for measuring the mass concentration of ambient particulate matter (PM).

2.2. Experimental setup and testing conditions

Fig. 2 shows the schematic diagram of experimental setup in this study. The setup included a large cylindrical test chamber (with the inner diameter, ID, of 30 cm), made of Plexiglass. A 4" PVC four-way connector was installed at the top of test chamber for introducing test particle stream and make-up clean air (if required) into the chamber. Test particles, once generated, were injected in the top opening of four-way connector. Makeup air flow was drawn in the connector from both side openings after passing through HEPA filter cartridges. A perforated metal plate was placed in the position near the bottom of test chamber to have uniform flow in the chamber. Two exits were designed at the chamber base to withdraw out the chamber flow. A valve and three external pumps were included in the setup to vary the total flow rate in test chamber. Seven tubes, for either mounting test optical PM sensors or as sampling probes are evenly spaced in the test chamber. Four low-cost optical PM sensors are vertically mounted on four tubes with one end sealed. The other three tubes are applied as sampling tubes for DustTrak, PDM and reference TEOM, which were placed directly underneath the test chamber.

Three different types of aerosol generators were utilized to generate/airborne test particles. For test particles in the sub-micrometer size range, a custom-made Collison atomizer was used to produce droplets of different mean sizes by nebulizing solutions in different salt concentrations. Three different solutions, i.e., Sodium Chloride, SC; Methylene blue, MB; and Fluorescein sodium, FS, were also used to produce droplets of different composition. An up-drifting nebulizer was also applied to generate droplets with the size distributions of the same peak sizes, but different standard deviations as those produced by the Collison atomizer. Droplets, once generated, were then passed through a diffusion dryer (with silica gel as the desiccant) to completely vaporize solvents in droplets prior to entering the 4-way connector. For test particles in the super-micrometer size range, a dust disperser (TOPAS SAG 410/U) was applied to airboren test dusts, i.e., A2 fine dust (or Arizona road dust, ARD), and a mixed dust (i.e., ARD and 2.5% ASHRAE #1 test dusts). A SKC cyclone was installed at the downstream of dust disperser to remove dust particles with the sizes larger than 2.5 μm (in a majority of experimental runs). A bypass for the particle stream was also included in our setup to release a portion of test particle stream prior to entering the 4-way connector. The mass concentration of particles in the test chamber was varied by adjusting both flowrates of particle stream and clean makeup air entering the connector.

Before our calibration, the spatial uniformity of particle concentration in the test chamber was characterized via DustTrak by taking the sequential measurement of particles sampled from each of seven tubes. The variation of measured particle concentration readings was in general less than 10%.

In this study, all PM sensors were primarily evaluated under steady particle concentration conditions. In the last part of our study, we further studied the calibration of low-cost optical PM sensors under the calm air condition. For such calibration, test particles at desired high mass concentration were first filled up in the test chamber by flowing a stream of particles in high mass concentration in the chamber. External vacuum pumps and a particle generator were turn off once particles in high particle concentration was achieved in the test chamber. The mass concentration of particles in the test chamber was decayed as the function of time because of particle loss and general sampling flow of reference TEOM. The readings of low-cost optical PM sensors were taken until the mass concentration of test particles reduced to an undetectable level.

3. Result and discussion

In this study, we evaluated the performance of all selected PM sensors using polydisperse particles of different mass concentrations, mean sizes (D_p), geometrical standard deviation (σ_g), and compositions. The calibration of tested PM sensors was carried out under the conditions of steady-state particle mass concentration.

Note that the performance calibration of tested PDM is only reported herein in this article although it was included in our study (for the sake of paper saving). It is because that we obtained the same result in all our experimental runs when comparing the PDM readouts with reference TEOM readouts. A typical comparison of PDM and reference TEOM readings is shown in Fig. 3: a) in wide mass concentration range (0–1000 μg/m^3) and b) in low concentration range (0–300 μg/m3). In this particular case, ARD was used as test particles. Good agreement between the readouts of PDM and TEOM is clearly evidenced in Fig. 3a. However, the calibration data shown in Fig. 3b indicates that the PDM lost its detection sensitivity when the mass concentration of ARD was less than 300 μg/m^3. The loss of detection sensitivity in low particle mass concentration for PDM is not a surprise given the consideration of its use of a

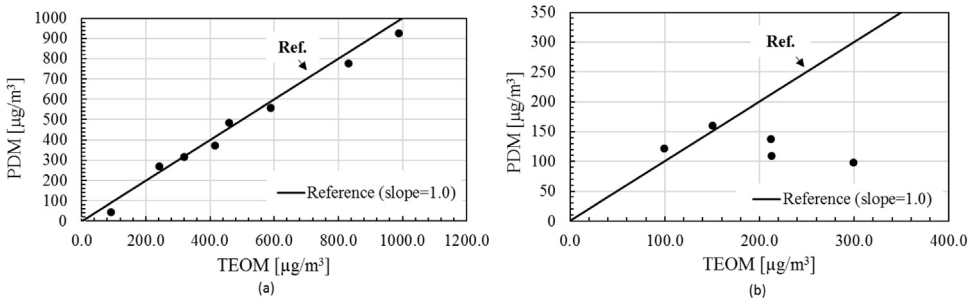

Fig. 3. Comparison of PDM and TEOM readouts: (a) in high concentration range; (b) in the low concentration range.

deformed metal tube as the oscillating element.

3.1. Effect of peak particle size

Test polydisperse particles in both sub-micrometers and super-micrometers were produced for this evaluation. For test particles in sub-micrometers, a custom-made Collison atomizer was applied to generate test particles by atomizing sodium chloride (NaCl) solutions in different volumetric concentrations. According to the measurement by the scanning mobility particle sizer (SMPS: TSI DMA 3081 with the platform model 3080), the number-based mean particle sizes, D_p, of test particles generated were 70, 86 and 95.0 nm, resulted from atomizing sodium chloride solutions of 0.1%, 0.5% and 1.0% by mass, respectively. To generate test particles in super-micrometers, ARD was airborne by a TOPAS powder disperser. Two different samples of test particles were used in this part of the calibration: one particle sample was obtained after passing through the SKC cyclone (to remove ones in the sizes larger than 2.5 μm) and the other sample obtained without the cyclone in the setup.

Fig. 4 shows the calibration of four low-cost optical PM sensors (i.e., Sharp, Shinyei, Samyoung and Oneair) and TSI DustTrak under the challenging of sub-micrometer-sized NaCl particles having three different peak sizes but the same geometrical standard deviation. As evidenced, the readouts of four low-cost optical PM sensors and DustTrak were linearly increased as the mass concentration of test particles was increased (under the tested particle mass concentration less than 1000 μg/m^3). The calibration lines of four low-cost optical sensors were, however, different from that of DustTrak. For the same particle mass concentration, the readouts of all four low-cost sensors were higher when tested with particles having larger peak sizes. The above trend was not observed for DustTrak. The above difference in the PM sensor performances might be due to different light sources and optical arrangements in all

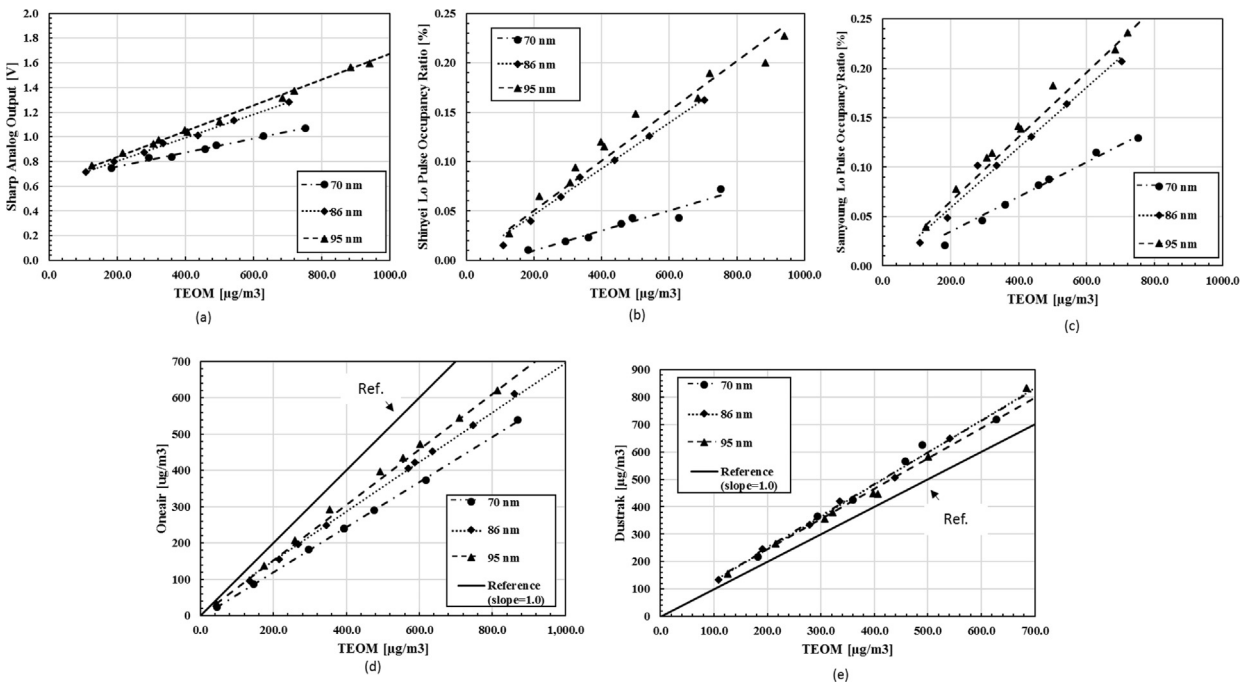

Fig. 4. Calibration of optical PM sensors under the challenge of submicrometer-sized particles in the size distribution of different mean particle sizes (the geometrical standard deviation and composition of test particles are fixed): (a) for Sharp sensor; (b) for Shinyei sensor; (c) for Samyoung sensor; (d) for Oneair sensor; (e) for TSI DustTrak.

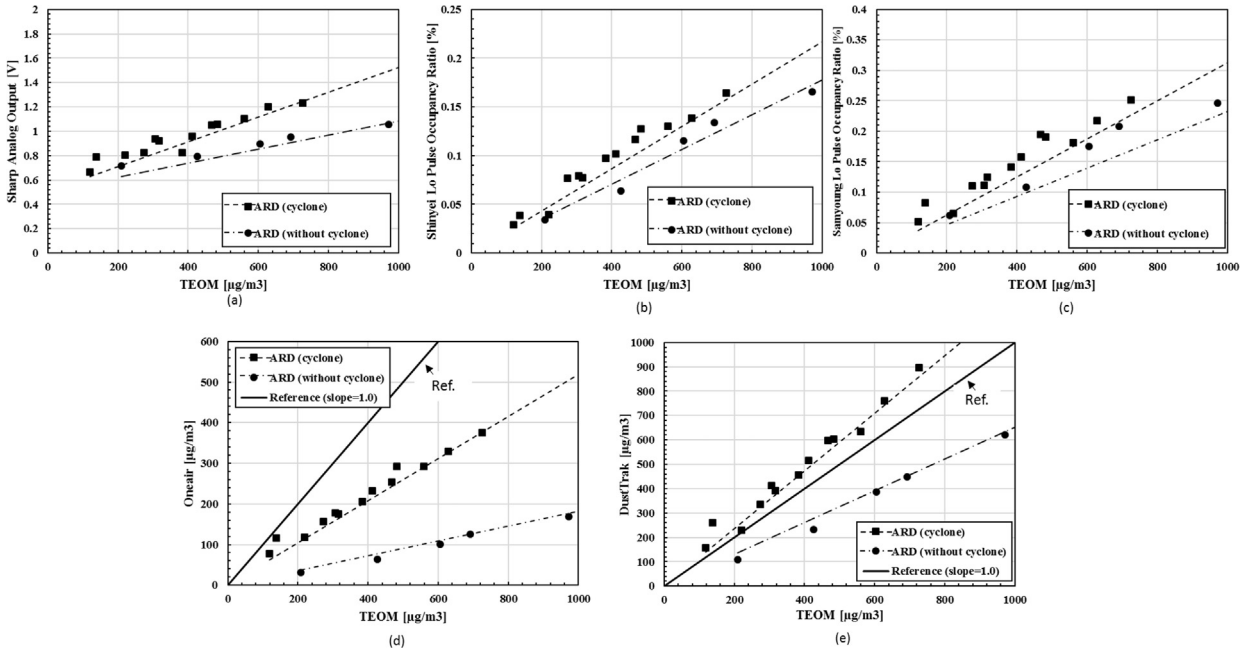

Fig. 5. Performance of optical PM sensors under the testing of supermicrometer-szied particles with different mean particle size while keeping the same for geometrical standard deviation and composition): (a) for Sharp sensor; (b) for Shinyei sensor; (c) for Samyoung sensor; (d) for Oneair sensor; (e) for TSI DustTrak.

optical PM sensors and DustTrak. An infrared emitting diode (with the wavelength of ~900 nm) was used as the light source in all four low-cost PM sensors. DustTrak, on the other hand, uses a laser diode with the wavelength of 655 nm as the source. Lights with shorter wavelengths enable DustTrak to measure particles of smaller sizes. A spherical mirror also was applied in DustTrak to collect scattered photons in a wide scattering angle and to focus them onto the photodetector. The above arrangement makes DustTrak less dependent on the mean size of test particles when compared with the performances of low-cost optical PM sensors. It is worth noting that, although the readout of DustTrak was negligibly dependent on the mean sizes of submicrometer-sized test particles, its mass reading was not the same as that of the reference TEOM (i.e., the slope of calibration line is not 1.0). The readout of DustTrak is higher than that of reference TEOM (by ~20%).

Fig. 5 gives the calibration of four low-cost PM sensors and DustTrak under the challenge of super-micrometer particles. It is found that the slopes of calibration lines for all given PM sensors in the cases without particles in sizes larger than 2.5 μm were higher than those in the cases with particles in sizes larger than 2.5 μm. At the first look, the above finding is contradictory to what expected via

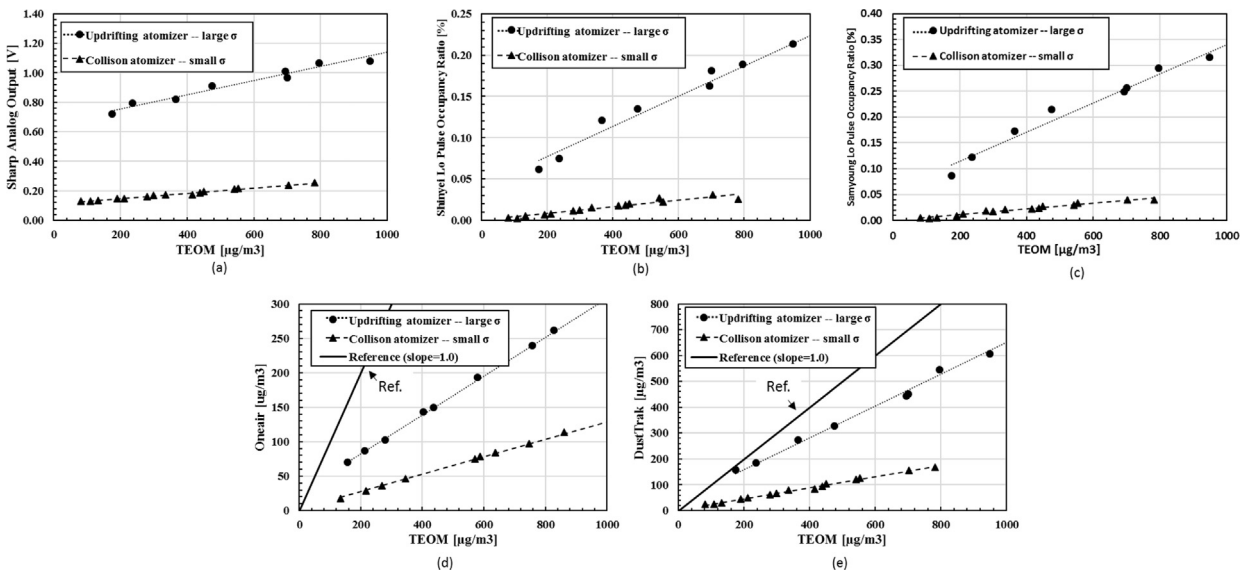

Fig. 6. Performance of optical PM sensors under the testing of particles having different standard deviation values in size distributions (while keeping the particle composition and mean size the same): (a) for Sharp sensor; (b) for Shinyei sensor; (c) for Samyoung sensor; (d) for Oneair sensor; (e) for TSI DustTrak.

the light scattering principle when large particles were present in the sensing volumes of low-cost optical PM sensors. The possible explanation for the above observation might be partially due to the sampling for low-cost optical PM sensors. Due to the inertia effect, particles with large sizes typically require a high flowrate to sample them into the sensing volumes of particle sensors. Gentle flow, moved by either the temperature gradient or a small fan in low-cost optical PM sensors, makes it difficult to sample large particles through their sensing volumes. Further, a small portion of large particles might be lost in the transport tubing for DustTrak. On the other hand, the iso-kinetic sampling was achieved for the reference TEOM to ensure the proper particle mass concentration measurement. As a result, the slopes of calibration lines for all the tested PM sensors are lower in the cases with large particles when compared with those in the cases without particles larger than 2.5 μm in sizes.

3.2. Effect of geometrical standard deviation

Two aerosol generators (i.e., custom-made Collison atomizer and updrifting nebulizer) were applied in this part of calibration to produce test particles having the same mean size of 76 ± 2 nm but different geometrical standard deviations (i.e., 1.802 and 2.486 respectively). The geometrical standard deviations of test particles were measured by TSI SMPS.

Fig. 6 shows the performance calibration of all optical PM sensors when challenged by the above two samples of test particles. Notice that shown in the above figure is the normalized readouts as a function of the reference TEOM reading, instead of raw PM sensor readouts. The above normalization of PM readouts is because of different number concentrations of two test particle samples. As shown in Fig. 6, the slopes of calibration lines for both test particle samples are again different. The larger the value of geometrical standard deviation of test particle samples, the higher the sensors' readouts. The above observation might be explained by the fact that more large particles are present in the test sample having a wide size distribution (i.e., large geometrical standard deviation value) compared to those in the test sample with a narrow size distribution. As a result, more particles of large sizes are present in sensing volumes of low-cost optical PM sensors when challenged with sample particles in a wide size distribution, resulting in more photon scattering.

A rough analysis was also carried out to understand the observed significant effect of geometrical standard deviation of particles. In this analysis, the light scattering from two samples of lognormal-size-distributed particles having the same total number concentration and peak size but two difference values of geometrical standard deviation (i.e., 1.8 and 2.5) were calculated. We assumed the wavelength of light source was 880 nm. The analysis further assume single particle scattering (i.e., no multiple light scattering) and 100% scattered light collection and detection. The Mie scattering program was used to compute the intensity of scattered light for particles in each size bin. The total scattered light was obtained by summing up the intensity in all the size bins. The above analysis shows that the total scattered intensity from the particle sample having the geometrical standard deviation of 2.5 was a factor of 8 higher than that from particles with the geometrical standard deviation of 1.8. Under the consideration of multiple light scattering, multiple wavelengths of LED sources, and partial scattering angle light collection and detection, the above factor should be lower in the experimental observation. Indeed, a factor of 6 in the readouts was found in this part of calibration.

3.3. Effect of particle composition

The material effect on the readouts of optical PM sensors was assessed using polydisperse submicrometer and supermicrometer particles of different compositions. For polydisperse submicrometer particles, the custom-made Collison atomizer was applied to produce them in three different compositions by spraying solutions of Methylene Blue (MB), Fluorescein Sodium (FS) and Sodium chlorine (NaCl), and completely evaporating solvents in generated droplets. The refractive indexes of MB, FS and NaCl at the red light wavelength are 1.55-0.6i, 1.364 and 1.544, respectively (Hinds, 1999). The calibration lines for four low-cost PM sensors and DustTrak are given in Fig. 7. It is not a surprise that the composition of test particles has significant effect on the readouts of all optical PM sensors. The similar trend on the material dependence was observed in the performances of three low-cost optical PM sensors (i.e., Sharp, Shinyei and Samyoung): the highest slope of calibration lines is found in the cases with MB particles, lower slope for FS particles, and the lowest for NaCl particles. However, the calibration line slopes for both Oneair and DustTrak are the highest in the cases with FS particles and the lowest remain in the cases with NaCl particles. The above finding of the performance difference on the material dependence could be due to optical designs and the calibration curve of tested PM sensors.

In addition, we also dispersed ARD and a mix of ARD-ASHRAE #1 test dust (2.5%) in air to evaluate the optical PM sensor performance. Both samples of test particles were passed through the SKC cyclone to remove those with the sizes larger than 2.5 μm. The calibration result of studied PM sensors using the ARD and the particle mix is given in Fig. 8. Again, the effect of particle material on the readouts of optical PM sensors was noticeable for super-micrometer particles of different compositions. At the same particle mass concentration, the readouts for all test optical PM sensors were higher when challenged with the mixed particles compared to those in the cases with ARD only.

3.4. Performance calibration under steady and transient particle mass concentration conditions

Because of no/low sampling flowrates for three low-cost PM sensors (i.e., Sharp, Shinyei and Samyoung Sensors), it is worthwhile to compare the calibration results under the conditions of steady and transient particle mass concentration. In this last part of our investigation, we further evaluated the performance of optical PM sensors in calm air. In this part of experiment, the test chamber was first filled up with test particles in desired mass concentration by flowing test particles in test chamber and varying the makeup air flowrate. Once the particle mass concentration reached its steady state, the aerosol generator and vacuum pumps were turn off in the

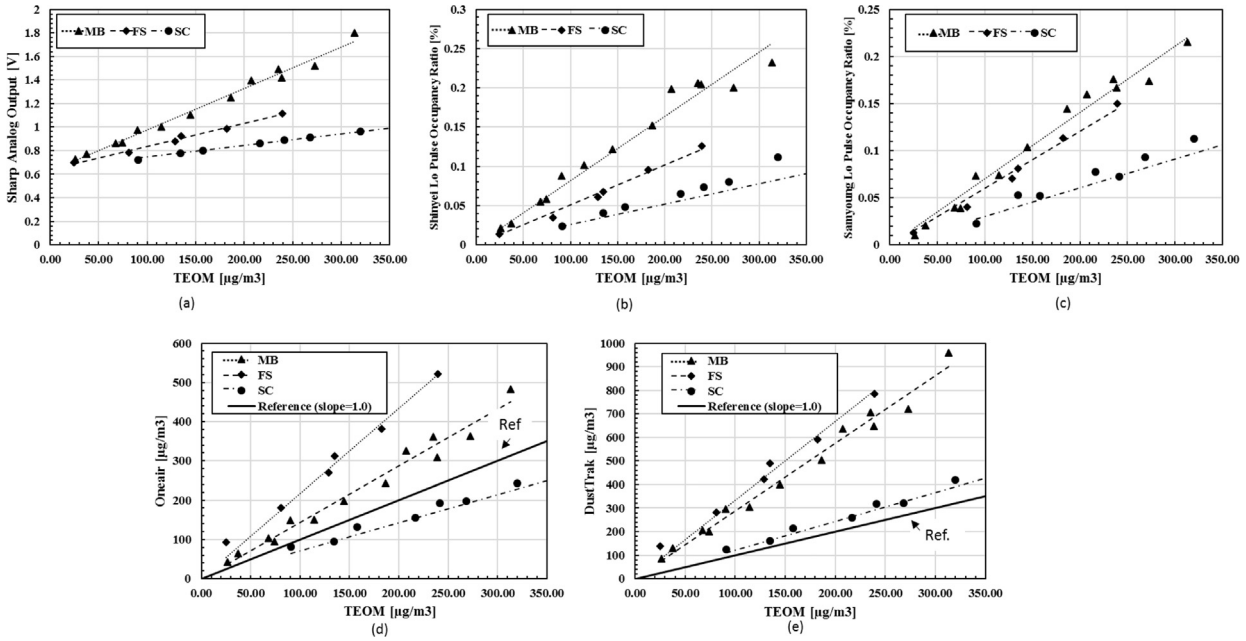

Fig. 7. Performance of optical PM sensors under the testing of submicrometer-sized particles in three different compositions while keeping the mean size and geometrical standard deviation of size distributions constant: (a) for Sharp sensor; (b) for Shinyei sensor; (c) for Samyoung sensor; (d) Oneair sensor; (e) for TSI DustTrak.

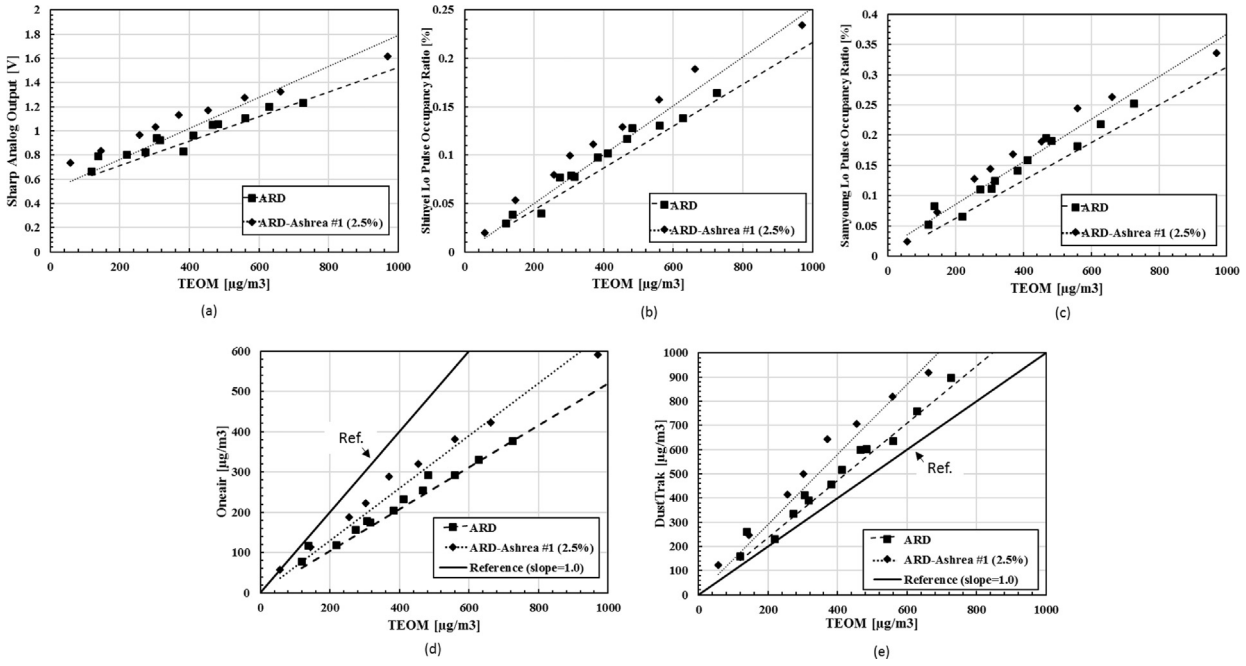

Fig. 8. Performance of optical PM sensors under the testing of supermicrometer-sized particles in two different composition: (a) for Sharp sensor; (b) for Shinyei sensor; (c) for Samyoung sensor; (d) Oneair sensor; (e) for TSI DustTrak.

calm air testing. The particle mass concentration in the test chamber were slowly decreased because of particle loss and minor sampling flow driven by the reference TEOM. Submicrometer-sized NaCl particles were used in this testing.

Fig. 9 shows the calibration result of the above three low-cost optical PM sensors under both calm air and steady-state particle mass concentration conditions. The given data shows that the readout of Sharp PM sensor maintains its linear calibration line at the particle concentration up to 1600 μg/m^3 but the linearity of readouts for both Shinyei and Samyoung sensors was deteriorated as the increase of mass concentration.

It is also found that the slopes of Shinyei and Samyoung sensor calibration curves obtained under the calm air condition were in

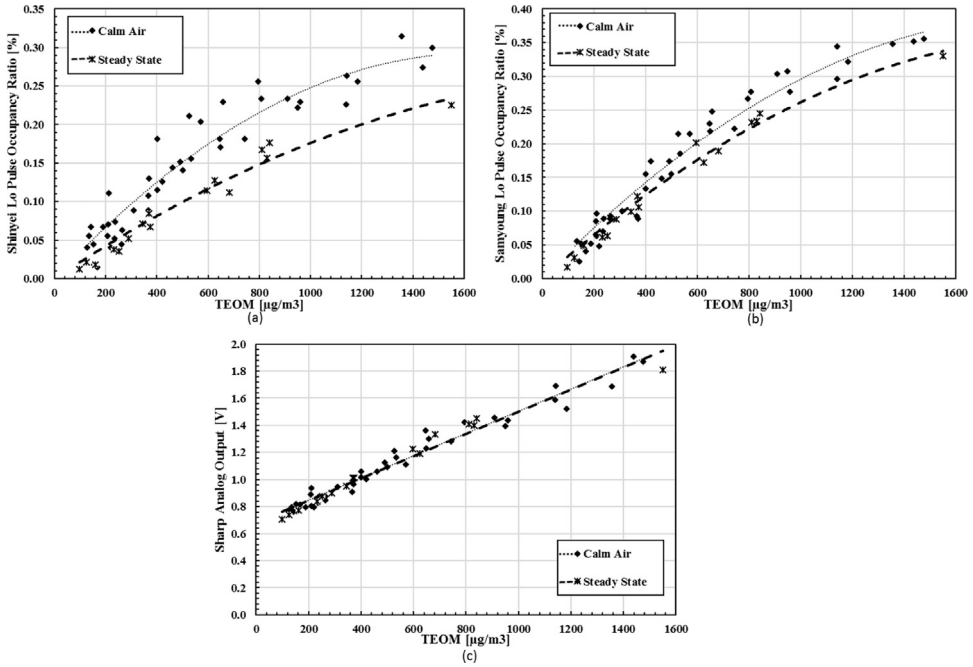

Fig. 9. Comparison of the performance of low-cost optical PM sensors under the conditions of steady and transient particle mass concentrations: (a) for Samyoung sensor; (b) for Shinyei sensor; (c) for Sharp sensor.

general higher than those obtained under the steady particle mass concentration condition while the difference for the Sharp sensor was negligible. The above finding might be partially attributed to the particle transport passage in both Shinyei and Samyoung sensors, having dead space in their passages. In the calm air testing, the test chamber and particle passages of low-cost PM sensors were initially filled up with particles in high concentration. Particles might be trapped in the dead space of particle passages inside Shinyei and Samyoung sensors. Because of slow sampling flow in both sensors, much longer time was needed to synchronize the particle concentration in the dead spaces with that in the ambient. The above possibility could explain the high readouts of these two sensors when calibrated under calm air condition compared to those under steady particle mass concentration condition. The difference in the readouts under two testing conditions was not observed for Sharp sensor. It is because of its simple, straight-through particle passage and our use of diffusive submicrometer-sized particles.

4. Conclusion

The performance of six PM sensors, including five optical and one mechanical PM sensors, i.e., Sharp, Shinyei, Samyoung, Oneair, TSI DustTrak and Personal Dust Monitor (PDM), were calibrated under the steady particle mass concentration condition and using lab-generated particles of various physical and chemical properties, i.e., total mass concentration, peak size, geometrical standard deviation of particle size distribution, and particle composition. The scientific TEOM (Model 1405) was selected as the reference in this calibration. Our calibration result shows that the readouts of all test PM sensors are in the linear relationship with the particle mass concentration when challenged by particles having the fixed size distribution and composition. The response of PDM in general agrees well with the readout of reference TEOM for a particle mass concentration higher than 0.3 mg/m^3. The PDM lost its detection sensitivity for particles in the mass concentration less than 0.3 mg/m^3 because of the use of deformed metal tube as the oscillating element in a PDM. However, the readouts of all tested optical PM sensors are sensitive to the physical and chemical properties of test particles. In the cases without the sampling issue, the increase of mean particle size and standard deviation in the size distribution of test particles in the same material resulted in the readout increase for optical PM sensors. The composition of test particles (i.e., refractive index) also have significant effect on the readouts of optical PM sensors. The level of composition effect depends on the optical design of PM sensors. Our study further demonstrated that the calibration of low-cost optical PM sensors should be performed under the steady particle concentration condition, instead of the transient particle mass concentration condition even at very slow transient conditions (i.e., under calm air condition). It might be due to the presence of dead space in the particle passages of low-cost optical PM sensors. It is thus concluded that the proper interpretation of readouts from low-cost optical PM sensors requires users to calibrate them using representative ambient particles (which is often unknown) and under the steady-state particle mass concentration. The potential sampling issue in the use of low-cost PM sensors should be also taken into the consideration when measuring large particles in the ambient.

Acknowledgement

The authors, Liu and Chen, are grateful for the partial financial support provided by the STAR program, US EPA (Grant # 83513201).

References

Alder, J. F., & McCallum, J. J. (1983). Piezoelectric crystals for mass and chemical measurements. A review. *Analyst*, *108*(1291), 1169–1189.
Austin, E., Novosselov, I., Seto, E., & Yost, M. G. (2015). Laboratory evaluation of the shinyei PPD42NS low-cost particulate matter sensor. *PLoS One*, *10*(9), e0137789.
Borm, P. J., Schins, R. P., & Albrecht, C. (2004). Inhaled particles and lung cancer, part B: Paradigms and risk assessment. *International Journal of Cancer*, *110*(1), 3–14.
Brook, R. D., Rajagopalan, S., Pope, C. A., Brook, J. R., Bhatnagar, A., Diez-Roux, A. V., ... Council on Nutrition and Metabolism, P. A. (2010). Particulate matter air pollution and cardiovascular disease. An update to the scientific statement From the American Heart Association. *Circulation*.
Cohen, A. J., & Pope, C. A. (1995). Lung cancer and air pollution. *Environmental Health Perspectives*, *103*(Suppl 8), 219–224.
Dockery, D. W., Pope, C. A., Xu, X., Spengler, J. D., Ware, J. H., Fay, M. E., ... Speizer, F. E. (1993). An association between air pollution and mortality in six U.S. cities. *New England Journal of Medicine*, *329*(24), 1753–1759.
Evans, J., van Donkelaar, A., Martin, R. V., Burnett, R., Rainham, D. G., Birkett, N. J., & Krewski, D. (2013). Estimates of global mortality attributable to particulate air pollution using satellite imagery. *Environmental Research*, *120*, 33–42.
Fan, J., Li, S., Fan, C., Bai, Z., & Yang, K. (2015). The impact of PM2.5 on asthma emergency department visits: A systematic review and meta-analysis. *Environmental Science and Pollution Research*, *23*(1), 843–850.
Gao, M., Cao, J., & Seto, E. (2015). A distributed network of low-cost continuous reading sensors to measure spatiotemporal variations of PM2.5 in Xi'an, China. *Environmental Pollution*, *199*, 56–65.
Hinds, W. C. (1999). *Aerosol technology: Properties. behaviour, and measurement of airborne particles*. New York: Wiley.
Holstius, D. M., Pillarisetti, A., Smith, K. R., & Seto, E. (2014). Field calibrations of a low-cost aerosol sensor at a regulatory monitoring site in California. *Atmospheric Measurement Techniques*, *7*(4), 1121–1131.
Knaapen, A. M., Borm, P. J., Albrecht, C., & Schins, R. P. (2004). Inhaled particles and lung cancer. Part A: Mechanisms. *International Journal of Cancer*, *109*(6), 799–809.
Krewski, D. (2009). Evaluating the effects of ambient air pollution on life expectancy. *New England Journal of Medicine*, *360*(4), 413–415.
Norris, G., YoungPong, S. N., Koenig, J. Q., Larson, T. V., Sheppard, L., & Stout, J. W. (1999). An association between fine particles and asthma emergency department visits for children in Seattle. *Environmental Health Perspectives*, *107*(6), 489–493.
Nyberg, F., Gustavsson, P., Järup, L., Bellander, T., Berglind, N., Jakobsson, R., & Pershagen, G. (2000). Urban air pollution and lung cancer in Stockholm. *Epidemiology*, *11*(5), 487–495.
Patashnick, H., & Rupprecht, E. G. (1991). Continuous PM-10 measurements using the tapered element oscillating microbalance. *Journal of the Air & Waste Management Association*, *41*(8), 1079–1083.
Potera, C. (2014). Toxicity beyond the Lung: Connecting PM(2.5), Inflammation, and Diabetes. *Environmental Health Perspectives*, *122*(1) (A29-A29).
Roessler, D. M. (1982). Diesel particle mass concentration by optical techniques. *Applied Optics*, *21*(22), 4077–4086.
Sousan, S., Koehler, K., Thomas, G., Park, J. H., Hillman, M., Halterman, A., & Peters, T. M. (2016). Inter-comparison of low-cost sensors for measuring the mass concentration of occupational aerosols. *Aerosol Science and Technology*, *50*(5), 462–473.
Tie, X., Wu, D., & Brasseur, G. (2009). Lung cancer mortality and exposure to atmospheric aerosol particles in Guangzhou, China. *Atmospheric Environment*, *43*(14), 2375–2377.
Wang, Y., Li, J., Jing, H., Zhang, Q., Jiang, J., & Biswas, P. (2015). Laboratory evaluation and calibration of three low-cost particle sensors for particulate matter measurement. *Aerosol Science and Technology*, *49*(11), 1063–1077.